Organic & Biomolecular Chemistry

ROYAL SOCIETY OF CHEMISTRY

PAPER

View Article Online
View Journal

Cite this: DOI: 10.1039/d1ob00536g

Distiboranes based on *ortho*-phenylene backbones as bidentate Lewis acids for fluoride anion chelation†

Di You, Benyu Zhou, Masato Hirai and François P. Gabbaï *

As part of our efforts in the chemistry of main group platforms that support anion sensing and transport, we are now reporting the synthesis of anitmony-based bidentate Lewis acids featuring the *o*-C_6F_4 backbone. These compounds can be easily accessed by reaction of the newly synthesized *o*-$C_6F_4(SbPh_2)_2$ (**5**) with *o*-chloranil or octafluorophenanthra-9,10-quinone, affording the corresponding distiboranes **6** and **7** of general formula *o*-$C_6F_4(SbPh_2(diolate))_2$ with diolate = tetrachlorocatecholate for **6** and octafluorophenanthrene-9,10-diolate for **7**, respectively. While **6** is very poorly soluble, its octafluorophenanthrene-9,10-diolate analog **7** readily dissolves in CH_2Cl_2 and undergoes swift conversion into the corresponding fluoride chelate complex [**7**-μ_2-F]$^-$ which has been isolated as a [^{n}Bu$_4$N]$^+$ salt. The *o*-C_6H_4 analog of **7**, referred to as **8**, has also been prepared. Although less Lewis acidic than **7**, **8** also forms a very stable fluoride chelate complex ([**8**-μ_2-F]$^-$). Altogether, our experiental results, coupled with computational analyses and fluoride anion affinity calculations, show that **7** and **8** are some of the strongest antimony-based fluoride anion chelators prepared to date. Another notable aspect of this work concerns the use of the octafluorophenanthrene-9,10-diolate ligand and its ablity to impart advantageous solubility and Lewis acidity properties.

Received 19th March 2021,
Accepted 30th April 2021

DOI: 10.1039/d1ob00536g

rsc.li/obc

Introduction

The chemistry of bidentate Lewis acids continues to garner significant interest in the area of anion sensing[1,2] and transport.[3] The advantageous properties of these compounds are typically correlated to the juxtaposition of the two Lewis acidic centres, facilitating anion chelation. A vast collection of constructs has been explored over the past decades as nicely documented in a series of reviews.[4] One of our contributions to this research effort has targeted bidentate systems in which the Lewis acidic centres are pentavalent antimony atoms.[5–8,9] We were motivated to engage in this research direction by the superior Lewis acidic properties of antimony(v) compounds.[10] Such properties have been extensively documented in the case of the pentahalides which have, for example, been used to access super acids.[11] We will also note that several recent contributions use SbF_5 as a benchmark for Lewis superacidity.[12,13] Our investigations in antimony(v) chemistry have generated organo-antimony Lewis acids that can be used as anion sensors,[14] and anion transporters.[15] As mentioned above, we have also synthesized bidentate antimony Lewis acids including the 9,9-dimethylxanthene-4,5-diyl derivative **1** which forms a very stable fluoride chelate complex (Scheme 1).[6] Inspection of the structure of [**1**-μ_2-F]$^-$ suggested that the presence of an electron-rich oxygen atom could lead to Pauli repulsion with the fluoride anion thus lowering the anion affinity of the bidentate chela-

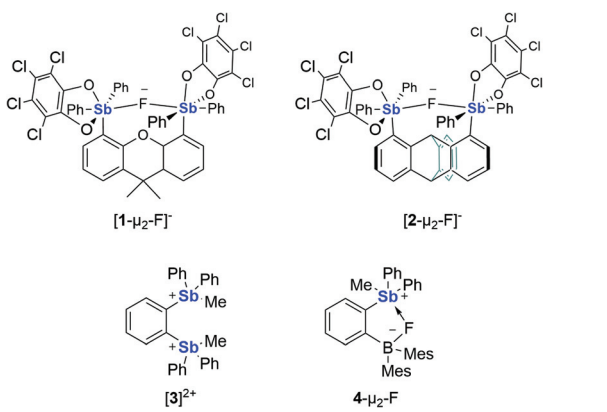

Scheme 1 Structure of known antimony(v) Lewis acids. The fluoride adducts are shown for **1**, **2** and [**4**]$^+$.

Department of Chemistry, Texas A&M University, College Station, TX 77843, USA. E-mail: francois@tamu.edu

† Electronic supplementary information (ESI) available: Additional experimental and computational details and crystallographic data in cif format. CCDC 2071279–2071284. For ESI and crystallographic data in CIF or other electronic format see DOI: 10.1039/d1ob00536g

tor. To circumvent this issue, we investigated the triptycene-1,8-diyl system **2** and observed that it displays a higher fluoride anion affinity than **1** (Scheme 1).[7]

To continue exploring how the backbone informs the properties of these bidentate antimony Lewis acids, we have now decided to investigate the synthesis and properties of analogues of **1** and **2** in which the two antimony moieties are connected by an electron-deficient tetrafluoro-*ortho*-phenylene backbone. Although this backbone has been previously employed for the design of bifunctional group 12[16] and 13 Lewis acids,[17,18] related systems incorporating antimony(v) as the Lewis acid have not been described. The most closely related systems include the non-fluorinated derivatives $[\mathbf{3}]^{2+}$ and $[\mathbf{4}]^{+}$ that we have investigated for catalysis in the case of $[\mathbf{3}]^{2+}$ and anion binding in the case of $[\mathbf{4}]^{+}$ (Scheme 1).[5,9]

Results and discussion

Using the strategy that we employed to access **1** and **2**, we first synthesized 1,2-bis(diphenylstibino)tetrafluorobenzene (**5**) in view of its reaction with *o*-chloranil. This new distibine could be obtained by reaction of 1,2-dibromotetrafluorobenzene with *n*-BuLi in THF at −65 °C followed by treatment with diphenylantimony chloride. Compound **5** was purified by column chromatography and isolated as a white crystalline solid. The formation of a single tetrafluoro-*o*-phenylene species was confirmed by ^{19}F NMR spectroscopy, which showed two resonances at −113.99 and −153.42 ppm in the expected 1 : 1 ratio. The ^{1}H NMR spectrum of **5** only displays resonances corresponding to the phenyl rings, which all appear equivalent in solution. This derivative was subsequently treated with two equivalents of *o*-chloranil in CH_2Cl_2 (Scheme 2). The reaction proceeded smoothly as indicated by *in situ* ^{19}F NMR spectroscopy which showed the emergence of two new signals at −120.6 ppm and −149.4 ppm assigned to the distiborane **6**. This new derivative was isolated as a pale yellow solid in 93% yield. However, once crystalized, it could not be brought back into solution. For this reason, **6** was not characterized by NMR spectroscopy. Yet, its composition was asserted by elemental analysis and its structure was determined by single crystal X-ray diffraction (*vide infra*). Confronted with the poor solubility of **6**, we decided to investigate the reaction of **5** with octafluorophenanthra-9,10-quinone (Scheme 2).[19] This reaction, which was carried out in CH_2Cl_2, afforded the desired distiborane **7** in less than an hour. After workup, this compound was isolated as a yellow solid. Gratifyingly, we found that **7** readily dissolves in THF and CH_2Cl_2. While the ^{19}F NMR spectrum of the octafluorophenanthra-9,10-quinone exhibits four resonances, the ^{19}F NMR spectrum of **7** shows ten peaks in CH_2Cl_2, consistent with the formation of a compound with C_2 symmetry (Fig. 1).

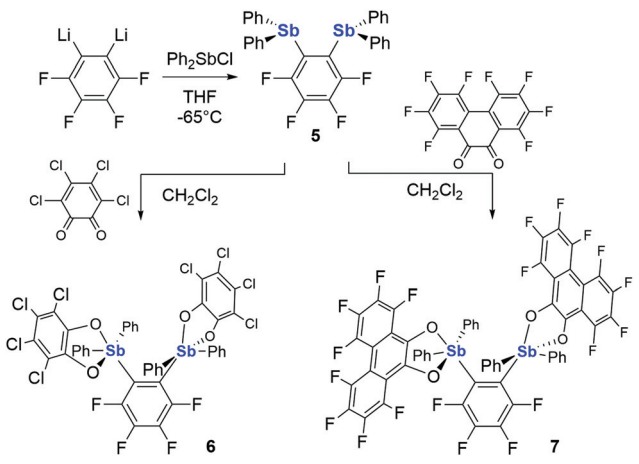

Scheme 2 Synthesis of **5**, **6**, and **7**.

We were able to obtain single crystals of **6** by layering a diethyl ether solution of *o*-chloranil with a CH_2Cl_2 solution of 1,2-bis(diphenylstibino)tetrafluorobenzene (Fig. 1). The crystal structure of **6** reveals that the compound has C_2 symmetry, with the two symmetry-equivalent antimony atoms separated by 3.8176(10) Å. The antimony atom adopts a distorted square pyramidal geometry with an average τ value = 0.14.[20] Square pyramidal geometries are not unusual for antimony(v) compounds including $(o\text{-}Cl_4C_6O_2)Sb(C_6F_5)_3$ which has a τ value of 0.32.[21] As indicated by the Sb1–O2a distance of 2.841(2) Å, the antimony atom and an oxygen atom of the neighbouring catecholate ligand are engaged in a donor–acceptor interaction. The structure of **7** has also been confirmed by single crystal X-ray diffraction which indicated the presence of two independent molecules in the asymmetric unit (Fig. 1). It is interesting to note that the distance separating the two antimony atoms in this compound (3.5665(7) Å/3.5942(7) Å) is notably shorter than in **6**. This shorter separation may be the result of increased O → Sb donor–acceptor bonding across the bidentate pocket. Indeed, **7** features intramolecular Sb···O distances in the 2.428(4)–2.642(5) Å range, some of which are distinctly shorter than in **6**. This significant shortening in **7** could be the result of an increased Lewis acidity of the antimony atoms and/or an increased Lewis basicity of the oxygen atoms.

To answer the above question, we computed the fluoride anion affinity of compounds **A** and **B** and found them to be both very close to each other although that of **B** appears slightly higher (Fig. 2).[22] This result indicates that if the octafluorophenanthrene-9,10-diolate ligand indeed elevates the Lewis acidity of antimony center, it does so only moderately. We will also note that the HOMO energy of **B** exceeds that of **A** by 0.48 eV. Since the HOMO spans the oxygen atoms of these derivatives, the Lewis basicity will likely be superior in the case of **B** which features the octafluorophenanthrene-9,10-diolate ligand. Thus, we propose that the increased basicity of the oxygen atoms in **7** is the dominating determinant responsible for the shortening of the intramolecular Sb···O distances. Finally, we note that the LUMO energy of these compounds are close to one another since they only differ by ~0.1 eV.

Compound **6** and **7** have also been investigated computationally using DFT methods. These calculations show that the LUMO of both compounds spans the two antimony atoms and displays dominant parentage from the σ* orbital of the Sb–

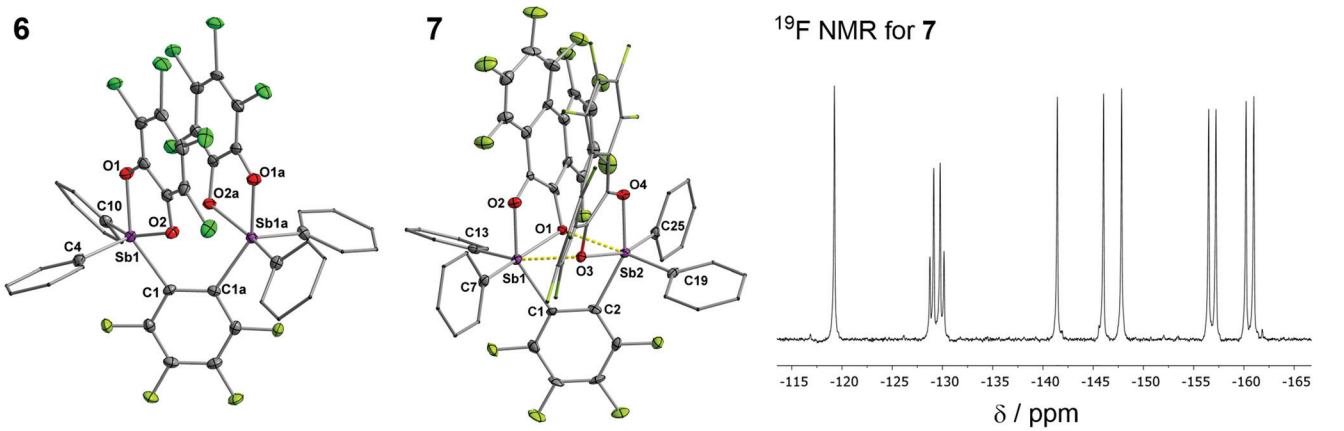

Fig. 1 Left: Crystal structures of **6** and **7**. Thermal ellipsoids are drawn at the 50% probability level. Parts of the molecules are shown as thin lines. In the case of **7**, only one of the two independent molecules is shown. Selected bond lengths (Å) and angles (°) for **6**: Sb1–Sb1a 3.8176(10), Sb1–O1 2.037(2), Sb1–O2 2.086(2), Sb1–O2a 2.841(2), O1–Sb1–O2 78.91(9), Sb1–C1–C1a 124.22(8). Selected bond lengths (Å) and angles (°) for **7**: Independent molecule 1. Sb1–Sb2 3.5666(7), Sb1–O3 2.572(5), Sb2–O1 2.428(4), O1–Sb1–O2 78.40(17), O3–Sb2–O4 78.43(17), Sb1–C1–C2 120.0 (5), Sb2–C2–C1 120.0(6). Independent molecule 2: Sb1′–Sb2′ 3.5942(7), Sb1′–O3′ 2.471(5), Sb2′–O1′ 2.642(5), O1′–Sb1′–O2′ 78.56(19), O3–Sb2–O4 78.49(18), Sb1–C1–C2 120.9(6), Sb2–C2–C1 120.6(6). Right: ^{19}F NMR spectrum of **7** recorded in CH_2Cl_2.

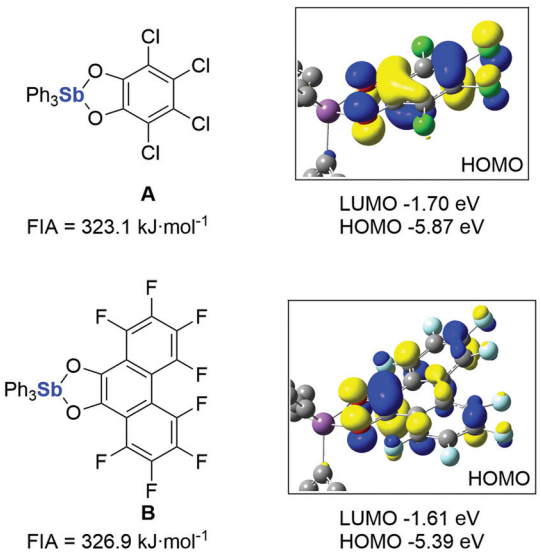

Fig. 2 Structures of the monofunctional model compounds, along with their computed fluoride anion affinities (FIA). The LUMO of each compound as well as their energies are also shown (isovalue = 0.04).

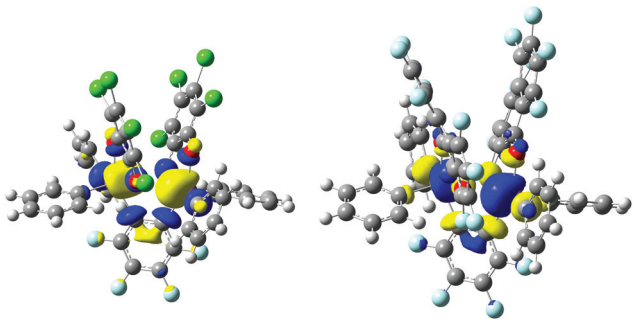

Fig. 3 Contour plot and energy of the LUMO of **6** (left) and **7** (right) (isovalue = 0.04).

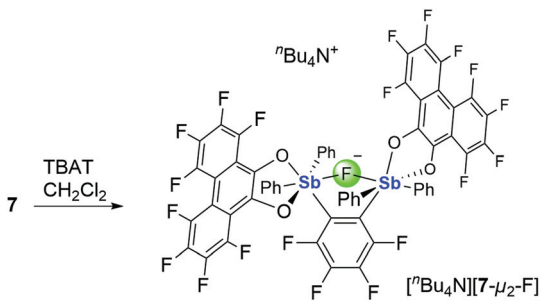

Scheme 3 Synthesis of [^{n}Bu$_4$N][7-μ_2-F].

C_{Phenyl} bond opposite to the open face of the antimony square pyramidal geometry (Fig. 3). The LUMO of **6** (−2.41 eV) and **7** (−2.38 eV) have very similar energies suggesting that the stronger intramolecular Sb → O interactions in **7** may have little effects on the Lewis acidity of the antimony centers.

Because of the poor solubility of **6**, we were not able to experimentally compare its Lewis acidity with that of **7**. Nonetheless, and encouraged by the solubility of **7**, we decided to explore its reaction toward the small fluoride anion. To this end, distiborane **7** was combined with [^{n}Bu$_4$N][Ph_3SiF_2] (TBAT) in CH_2Cl_2 (Scheme 3). Evaporation of the solvent and repeated washing of the residue with pentane, afforded pure [^{n}Bu$_4$N][7-μ_2-F] as a yellow solid in good yield. This salt has been characterized using NMR spectroscopy, single crystal X-ray diffraction and elemental analysis. The ^{19}F NMR spectrum of [^{n}Bu$_4$N][7-μ_2-F] displays nine resonances between −115 and −170 ppm, corresponding to the octafluorophenanthrene-9,10-diolate and the tetrafluoro-*ortho*-phenylene backbone. The observation of only nine reso-

nances indicates the accidental overlap of two magnetically inequivalent fluorine signals. The chelated fluoride anion appears at −77.1 ppm in $CDCl_3$. This value is close to that in $[Ph_3Sb(o\text{-}O_2C_6Cl_4)F]^-$ (−84.6 ppm)[6] or Ph_4SbF (−81.4 ppm);[23] yet it significantly differs from those in $[\mathbf{1}\text{-}\mu_2\text{-}F]^-$ (−25.6 ppm) and $[\mathbf{2}\text{-}\mu_2\text{-}F]^-$ (−26.4 ppm).[6,7] The formation of $[\mathbf{7}\text{-}\mu_2\text{-}F]^-$ shows that the intramolecular Sb → O donor–acceptor interactions in **7** are not sufficiently strong to quench the Lewis acidity of these derivatives.

Colourless single crystals of $[^nBu_4N][\mathbf{7}\text{-}\mu_2\text{-}F]$ were obtained by diffusing pentane into a CH_2Cl_2 solution of the salt. The crystal structure of $[^nBu_4N][\mathbf{7}\text{-}\mu_2\text{-}F]$ confirms the formation of a fluoride chelate complex with the bridging fluoride anion adopting a bent geometry as indicated by the value of the Sb–F–Sb angle of 129.48(6)° (Fig. 4). Such a bending is reminiscent of that observed in the fluoride adducts of bidentate diboranes.[1,17,24] We should also be reminded that the $[Sb_2F_{11}]^-$ anion may display a bent fluoride bridge as in the case of its hydronium salt where the Sb–F–Sb angles range from 149.4(3) to 145.9(2)°.[25] We reason that the accentuated bending of the Sb–F–Sb angle results from the rigid arrangement of the two Lewis acids. In support of this view, we will note that the larger spacing of the Lewis acids in $[\mathbf{1}\text{-}\mu_2\text{-}F]^-$ and $[\mathbf{2}\text{-}\mu_2\text{-}F]^-$ leads to significantly larger angles of 165.4(1)° and 174.4(1)°, respectively.[6,7] The Sb1–Sb2 separation of 3.8525(6) Å in $[^nBu_4N][\mathbf{7}\text{-}\mu_2\text{-}F]$ is notably increased when compared to that of the starting distiborane (av. 3.58 Å) owing to the disappearance of O → Sb bonding between the two distiborane units. The Sb–F bond lengths (2.1322(11) and 2.1275(11) Å) fall within the expected range and are comparable to those measured in $[\mathbf{1}\text{-}\mu_2\text{-}F]^-$ and $[\mathbf{2}\text{-}\mu_2\text{-}F]^-$.[6,7]

To complete this study and better understand the impact of perfluorination of the *ortho*-phenylene backbone, we targeted compound **8** which was obtained as a yellow crystalline solid by reaction of 1,2-bis(diphenylstibino)benzene[26] with two equivalents of octafluorophenthra-9,10-quinone in CH_2Cl_2 (Scheme 4). In the ^1H NMR of **8** in $CDCl_3$, the *o*-phenylene resonances appear as multiplets at 7.67 ppm while the phenyl group gives rise to a broad signal centred at 7.39 ppm. The ^{19}F NMR spectrum features five broad signals corresponding to the octafluorophenanthrene-9,10-diolate ligand, indicating that some of the fluorine resonances are overlapping. The crystal structure of distiborane **8** has been determined (see ESI†). The Sb–Sb separation of 3.568(3) Å and the short O → Sb contacts of 2.557(3) and 2.525(2) Å connecting the stiborane units are comparable to those in the structure of **7**, suggesting that the Lewis acidity of the antimony centers might be comparable (Fig. 5). This analogy carries forward in the behaviour

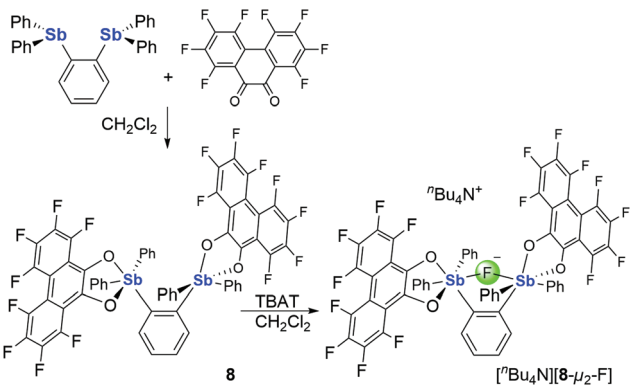

Scheme 4 Synthesis of **8** and $[^nBu_4N][\mathbf{8}\text{-}\mu_2\text{-}F]$.

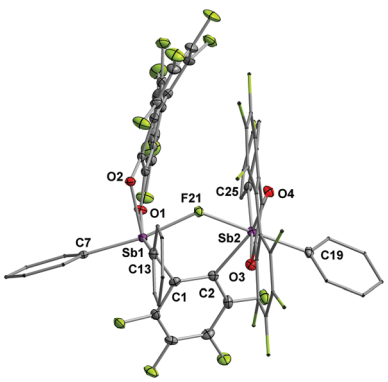

Fig. 4 Structure of $[^nBu_4N][\mathbf{7}\text{-}\mu_2\text{-}F]$ in the crystal. Thermal ellipsoids are drawn at the 50% probability level. The hydrogen atoms and the $[^nBu_4N]^+$ cation are omitted for clarity and the phenyl rings as well as one of the octafluorophenanthrene unit are shown as thin lines. Selected bond lengths (Å) and angles (°): Sb1–Sb2 3.8525(6), Sb1–C1 2.185(2), Sb1–O1 2.0570(14), Sb1–O2 2.0658(14), Sb2–C2 2.182(2), Sb2–O3 2.0615(14), Sb2–O4 2.0561(14), Sb1–F21–Sb2 129.48(6), O1–Sb1–O2 78.19(5), O3–Sb2–O4 78.94(5), F21–Sb1–C7 190.32(6), F21–Sb2–C19 169.98(6).

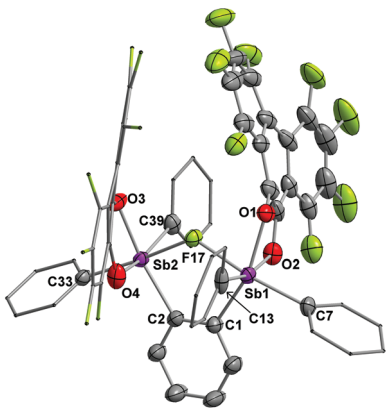

Fig. 5 Structure of $[^nBu_4N][\mathbf{8}\text{-}\mu_2\text{-}F]$ in the crystal. Thermal ellipsoids are drawn at the 50% probability level. The hydrogen atoms and the $[^nBu_4N]^+$ cation are omitted for clarity and the phenyl rings as well as one of the octafluorophenanthrene unit are shown as thin lines. Selected bond lengths (Å) and angles (°): Sb1–C1 2.150(4), Sb1–C7 2.146(5), Sb1–C13 2.126(5), Sb1–O1 2.064(3), Sb1–O2 2.064(3), Sb2–C2 2.143(4), Sb2–C33 2.138(4), Sb2–C39 2.125(5), Sb2–O3 2.060(3), Sb2–O4 2.066(3), Sb1–F17–Sb2 126.30(12), O1–Sb1–O2 77.79(13), C1–Sb1–C7 101.05(17), C1–Sb1–C13 102.3(2), C7–Sb1–C13 97.15(18), O3–Sb2–O4 76.67(15), C2–Sb2–C33 101.45(17), C2–Sb2–C39 102.94(19), C33–Sb2–C39 100.61(18).

of **8** towards fluoride since its reaction with TBAT affords [^{n}Bu$_4$N][**8**-μ_2-F] (Scheme 4). The appearance of eight distinct octafluorophenanthrene-9,10-diolate resonances in the ^{19}F NMR spectrum between −130 and −170 ppm and a single resonance for the bridging fluoride anion at −76.8 ppm confirmed the formation of an anionic chelate complex analogous to [**7**-μ_2-F]$^-$. In the crystal, the metrical parameters defining the geometry of the chelated fluoride anion in [**8**-μ_2-F]$^-$ (Sb–F = 2.129(3) and 2.140(3) Å, and Sb1–F17–Sb2 angle of 126.30(12)°) are again similar to those of [**7**-μ_2-F]$^-$ (Fig. 5).

Given that these experimental results did not allow us to clearly discern a notable difference in the Lewis acidity of **7** and **8**, we computed the fluoride anion affinity (FIA) of these two compounds using DFT methods. These calculations afforded an FIA of 399.7 kJ mol^{-1} for **7** which is higher than that of **8** (390.7 kJ mol^{-1}). These results show that perfluorination of the phenylene backbone moderately enhances the Lewis acidity of this anion chelating platform. Such results are consistent with those obtained with other bidentate Lewis acids including those containing mercury as the Lewis acidic element.[16] Finally, the FIAs of **7** and **8** are either comparable of slightly higher than those computed for **1** (365 kJ mol^{-1}) and **2** (395 kJ mol^{-1}) at the same level of theory.[6,7] This comparison shows that despite its simplicity, the *o*-phenylene backbone, fluorinated or not, is well adapted to the design of potent antimony-based anion chelators.

Aiming to get experimental verification for the elevated Lewis acidity of **7**, we decided to develop a resilience test in which [^{n}Bu$_4$N][**7**-μ_2-F] and [^{n}Bu$_4$N][**8**-μ_2-F], mixed in equimolar quantities, were concomitantly challenged by addition of Al(NO$_3$)$_3$ in THF (Fig. 6). Upon addition of the first equivalent of Al(NO$_3$)$_3$, [^{n}Bu$_4$N][**8**-μ_2-F] disappeared, while [^{n}Bu$_4$N][**7**-μ_2-F] remained intact. An additional equivalent of Al(NO$_3$)$_3$ led to the disappearance of [^{n}Bu$_4$N][**7**-μ_2-F]. These results agree with the computational finding that **7** has a higher fluoride affinity than **8**.

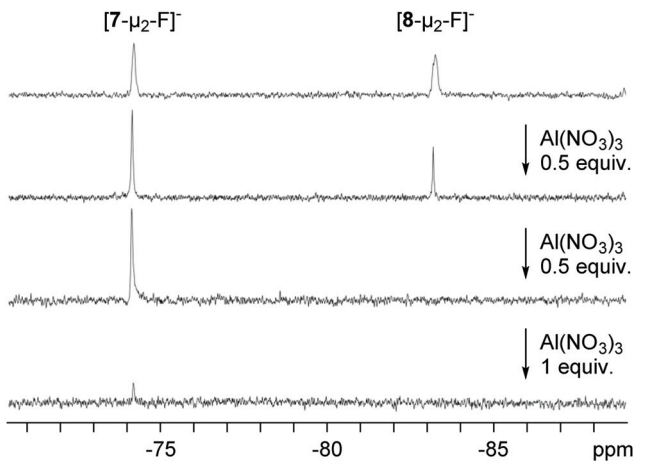

Fig. 6 ^{19}F NMR monitoring of a 1 : 1 mixture of [^{n}Bu$_4$N][**7**-μ_2-F] and [^{n}Bu$_4$N][**8**-μ_2-F] in THF upon incremental addition of Al(NO$_3$)$_3$.

Conclusions

Altogether this paper describes the synthesis of *o*-phenylene-based distiboranes as bidentate Lewis acids. These derivatives, which are obtained by oxidation of the corresponding distibine by addition of an *o*-quinone such as *o*-chloranil or octafluorophenanthra-9,10-quinone, readily chelate the fluoride anion as established in the case of the octafluorophenanthrene-9,10-diolate derivatives. The computed FIA of these derivatives suggest that they are some of the strongest antimony-based fluoride anion chelators prepared by our group, in particular when the *o*-tetrafluorophenylene group is employed. Finally, we propose that the most innovative aspect of this study relates to the use of octafluorophenanthrene-9,10-diolate as a chelating ligand. This ligand has, to our knowledge, never been employed and the results that we have obtained suggest that its use may lead to higher solubilities than those displayed by compounds containing the tetrachloro-catecholate ligand. The presence of NMR active ^{19}F nuclei on the backbone is also an attractive trait that facilitates spectroscopic monitoring of the chemistry. This result is of relevance to ongoing efforts aimed at the synthesis of catecholate main group derivatives as super acids.[13,27]

Experimental section

General considerations

Antimony is potentially toxic and should be handled with caution. Perfluoro(tetradecahydrophenanthrene) was purchased from Beantown Chemical, *n*-BuLi (2.65 M in hexane) from Alfa Aesar, tetrachloro-*o*-benzoquinone (*o*-chloranil) from Acros Organics, and TBAT form TCI. All commercially available chemicals were used as received. Ph_2SbCl[28] and 1,2-bis(diphenylstibino)benzene[5] were prepared by following or modifying previously reported procedures. All preparations were carried out under an atmosphere of dry N_2 employing either a glovebox or standard Schlenk techniques unless specified. Solvents were dried by passing through an alumina column (pentane and CH_2Cl_2) or by refluxing under N_2 over Na/K (hexanes, Et_2O, and THF). All other solvents were ACS reagent grade and used as received. NMR spectra were recorded on a Varian Unity Inova 400 FT NMR (399.508 MHz for ^{1}H, 100.466 MHz for ^{13}C) or a Varian Unity Inova 500 FT NMR (499.42 MHz for ^{1}H, 469.86 MHz for ^{19}F, 125.60 MHz for ^{13}C) spectrometer at ambient temperature. ^{1}H and ^{13}C NMR chemical shifts are given in ppm and are referenced against $SiMe_4$ using residual solvent signals as secondary standards. ^{19}F NMR chemical shifts are given in ppm and are referenced against $CFCl_3$ using BF_3•Et_2O as an external secondary standard assigned a chemical shift value of −153.0 ppm. Elemental analyses (EA) were performed at Atlantic Microlab (Norcross, GA).

Computational details

Density functional theory (DFT) structural optimizations with the Gaussian 09 program.[29] In all cases, the structures were

optimized using the B3LYP functional[30] and the following mixed basis sets: aug-cc-pVTZ-PP[31] for Sb, 6-311G(d)[32] for Cl, 6-31G(d')[33] for F, 6-31G[34] for C, O and H. When available, the experimentally determined geometry of the derivative was used as an initial guess for the optimization. These geometries are available under the CCDC deposition numbers listed in the following paragraph. For all optimized structures, frequency calculations were carried out to confirm the absence of imaginary frequencies. The molecular orbitals were visualized using GaussView 6.0. The enthalpies used to derive the FIA were obtained by single point calculations carried out at the optimized geometry with the B3LYP functional and the following mixed basis sets: aug-cc-pVTZ-pp for Sb and 6-311+g(2d,p) for C, H, O, and F. The enthalpy correction term was obtained from the above-mentioned frequency calculations.

Crystallographic measurements

The crystallographic measurements were performed at 110(2) K using a Bruker APEX-II CCD area detector diffractometer, with Mo-K_α radiations (λ = 0.71069 A). A specimen of suitable size and quality was selected and mounted onto a nylon loop. The semi-empirical method SADABS was applied for absorption correction. The structure was solved by direct methods, which successfully located most of the non-hydrogen atoms. Subsequent refinement on F^2 using the SHELXTL/PC package (version 6.1) allowed location of the remaining non-hydrogen atoms. All H-atoms were geometrically placed and refined using a standard riding model. CCDC 2071279 (**6**), 2071280 (**7**), 2071281 (**8**), 2071282 ([^{n}Bu$_4$N][**7**-μ_2-F]), 2071283 ([^{n}Bu$_4$N][**8**-μ_2-F]) and 2071284 (**B**)† contain the supplementary crystallographic data for this paper.

Synthesis of decafluorophenanthrene

The procedure is based on that previously reported.[19] A 100 mL Schlenk flask was charged with Cp_2TiCl_2 (0.312 g, 1.25 mmol), $HgCl_2$ (1.72 g, 6.33 mmol), aluminum powder (1.74 g, 64.5 mmol), and 30 mL of THF. A crystal of I_2 was subsequently added and the mixture was degassed. The solution color turned from red to dark yellow within 15 min, an indication of the formation of activated low-valent "Cp_2Ti" complex. The flask was refilled with N_2 and neat perfluoro(tetradecahydrophenanthrene) (4.06 g, 6.5 mmol) was slowly added using syringe over the course of 5 min. This addition led to an exothermic reaction. After stirring the mixture for 30 min and cooling it down to ambient temperature, the reaction mixture was degassed once again and the flask was refilled with fresh N_2. The resulting dark yellow slurry was periodically degassed (every 12 h) and refilled with N_2. After stirring for 3 days, the solution color turned to dark purple and the solvent was removed under vacuum. The residue was extracted with Et_2O (3 × 20 mL) and the remaining precipitate was removed by filtration over Celite. The red filtrate was concentrated and purified by silica gel column chromatography using hexanes as an eluent. Decafluorophenanthrene was obtained as a colorless solid in a 28% yield (644 mg, 1.8 mmol). The product formation was confirmed by ^{19}F NMR spectroscopy. ^{19}F NMR (375.84 MHz, $CDCl_3$): δ −125.58 (m; 2F), −144.00 (m; 2F), −144.88 (m; 2F), −151.08 (m; 2F), −152.55 (m; 2F).

Synthesis of octafluorophenthra-9,10-quinone

This compound was prepared based on a published procedure.[35] A 25 mL Schlenk tube was charged with decafluorophenanthrene (500 mg, 1.42 mmol) and oleum (20–24% SO_3; 10 mL) under N_2. The color immediately turned brown. The reaction was heated to 100 °C and stirred for 3 h. The brown mixture was poured onto ice and transferred to a separation funnel. After adding Et_2O (50 mL), the biphasic mixture was shaken and the two layers were separated. The aqueous layer was extracted with Et_2O (2 × 30 mL). The resulting organic phase were dried over anhydrous $MgSO_4$, and filtered through Celite. The filtrate was concentrated and was purified by silica gel (40 g) column chromatography. Hexanes was first used as an eluent before being mixed with CH_2Cl_2 in a 6 : 4 (v : v) ratio. Octafluorophenthra-9,10-quinone was obtained as a bright yellow crystalline solid in a 33% yield (162 mg). This compound is air stable and could be stored on the bench without special precaution. The product formation was confirmed by ^{19}F NMR spectroscopy. ^{19}F NMR (375.84 MHz, $CDCl_3$): δ −125.40 (m; 2F), −133.26 (m; 2F), −139.61 (m; 2F), −148.03 (m; 2F).

Synthesis of 5

A solution of *n*-BuLi in hexanes (3.5 mL, 2.2 M, 7.7 mmol) was added dropwise to a solution of 1,2-dibromotetrafluorobenzene (0.995 g, 3.22 mmol) in THF (20 mL) at −78 °C. After stirring at this temperature for 45 min, this solution was treated with Ph_2SbCl (2.00 g, 6.44 mmol) which was added *via* cannula transfer as a suspension in THF (10 mL). The solution was slowly warmed to ambient temperature and stirred for an additional 12 h. The solvent was removed under reduced pressure to afford a residue which was taken up in CH_2Cl_2 (30 mL). The resulting mixture was filtered through celite and brought to dryness under vacuum, resulting in a yellow oily product. Final purification *via* column chromatography with silica gel as a stationary phase and hexanes as an eluent afforded **5** as a colorless crystalline solid (1.41 g, 62.3%). ^{1}H NMR (499.42 MHz, $CDCl_3$): δ 7.46 (m, 8H, *m*-Sb*Ph*), 7.30–7.34 (m, 12H, *p*-Sb*Ph*, *o*-Sb*Ph*), ^{13}C{^{1}H} NMR (125.60 MHz, $CDCl_3$): δ = 149.52–151.74 (dm, $^1J_{C-F}$ = 260.9 Hz), 139.68–142.20 (dm, $^1J_{C-F}$ = 257.0 Hz), 137.73, 136.29, 129.10, 129.02. ^{19}F NMR (469.86 MHz, $CDCl_3$): δ −124.34 (d, 2F, $^3J_{F-F}$ = 18.9 Hz), −153.16 ppm (d, 2F, $^3J_{F-F}$ = 19.0 Hz). Elemental analysis calculated (%) for: C, 51.48; H, 2.88, found C, 51.27; H, 3.00.

Synthesis of 6

A CH_2Cl_2 solution (2 mL) of *o*-chloranil (35.3 mg, 0.140 mmol) was added dropwise to a stirred solution of **5** (50.2 mg, 0.0720 mmol) in CH_2Cl_2 (2 mL). Stirring this solution for 30 min produced a **6** as yellow solid which was isolated by filtration in a 93% yield (79.5 mg). Single crystals were obtained

as yellow blocks by layering a diethyl ether solution of *o*-chloranil with a CH_2Cl_2 solution of **5** at ambient temperature. ^{19}F NMR (469.86 MHz, THF): δ −120.59 (d, 2F, $^3J_{F-F}$ = 16.2 Hz), −149.41 ppm (d, 2F, $^3J_{F-F}$ = 16.2 Hz). Elemental analysis calculated (%) for $C_{42}H_{20}Cl_8F_4O_4Sb_2$-$CH_2Cl_2$: C, 40.45; H, 1.74, Cl, 27.77; found C, 40.66; H, 1.84; Cl, 27.39.

Synthesis of 7

A solution of **5** (78.0 mg, 0.111 mmol) in CH_2Cl_2 (2 mL) was slowly added to a solution of octafluorophenthra-9,10-quinone (78.4 mg, 0.220 mmol) in CH_2Cl_2 (2 mL). After stirring for 30 min, the resulting solution was brought to dryness under vacuum affording a residue that was washed with Et_2O (2 × 2 mL) and pentane (2 mL). This procedure afforded **7** as a yellow solid in 69% yield (108 mg). Single crystals were obtained by slow evaporation of a CH_2Cl_2 solution. ^1H NMR (499.42 MHz, $CDCl_3$): δ 7.93 (d, 4H, $^3J_{H-H}$ = 7.8 Hz), 7.73 (t, 2H, $^3J_{H-H}$ = 7.6 Hz), 7.32–7.23 (m, 4H), 7.40 (d, 4H, $^3J_{H-H}$ = 7.8 Hz), 7.29 (t, 2H, $^3J_{H-H}$ = 7.77 Hz), 7.20 ppm (t, 4H, $^3J_{H-H}$ = 7.8 Hz). $^{13}C\{^1H\}$ NMR (125.60 MHz, $CDCl_3$): 137.16, 135.44, 134.60, 133.13, 132.53, 131.87, 129.86, 129.58. ^{19}F NMR (469.86 MHz, CH_2Cl_2): −119.28 (s, 2F), −129.00 (pseudo q, 4F), −141.71 (s, 2F), −146.02 (s, 2F), −147.83 (s, 2F), −156.47 (s, 2F), −157.20 (s, 2F), −160.20 (s, 2F), −160.97 ppm (s, 2F). Elemental analysis calculated (%) for $C_{58}H_{20}F_{20}O_4Sb_2$: C, 49.61; H, 1.44; found C, 49.87; H, 1.64.

Synthesis of [^{n}Bu$_4$N][7-μ$_2$-F]

A solution of TBAT (22 mg, 0.041 mmol) in CH_2Cl_2 (2 mL) was slowly added to a solution of **7** (58 mg, 0.041 mmol) in CH_2Cl_2 (1 mL). After stirring for 30 min, the resulting solution was brought to dryness under vacuum affording an orange oil which was washed with a copious amount of pentane. This procedure afforded [^{n}Bu$_4$N][7-μ$_2$-F] in 80% yield (63 mg). Single crystals of [^{n}Bu$_4$N][7-μ$_2$-F] were obtained from CH_2Cl_2 upon diffusion of pentane. ^1H NMR (499.42 MHz, $CDCl_3$): δ 7.63 (d, 4H, J_{H-H} = 7.5 Hz), 7.39 (d, 4H, $^3J_{H-H}$ = 7.5 Hz), 7.17–7.08 (m, 6H), 6.90 (t, 4H, $^3J_{H-H}$ = 7.5 Hz), 6.82 (t, 2H, $^3J_{H-H}$ = 7.3 Hz), 2.72 (pseudo t, 8H, TBA–CH_2), 1.27 (broad, 8H, TBA–CH_2), 1.13 (m, 8H, TBA–CH_2), 0.82 (t, 12H, $^3J_{H-H}$ = 7.45 Hz, TBA–CH_3). $^{13}C\{^1H\}$ NMR (125.60 MHz, CD_2Cl_2): 135.31, 133.56, 133.09, 129.25, 128.85, 128.52, 127.98, 59.31, 24.19, 20.05, 13.68. $^{19}F\{^1H\}$ NMR (469.86 MHz, $CDCl_3$): −77.08 (s, 1F), −117.46 (s, 2F), −132.31 (pseudo q, 4F), −144.59 (s, 2F), −148.11 (s, 2F), −152.77 (s, 2F), −159.97 (s, 4F), −165.31(s, 2F), −165.64 (s, 2F). Elemental analysis calculated (%) for $C_{74}H_{56}F_{21}NO_4Sb_2$: C, 53.36; H, 3.39; N, 0.84; found C, 53.62; H, 3.53; N, 0.99.

Synthesis of 8

A solution of 1,2-bis(diphenylstibino)benzene (95 mg, 0.27 mmol) in Et_2O (3 mL) was slowly added to a solution of octafluorophenthra-9,10-quinone (83 mg, 0.13 mmol) in CH_2Cl_2 (0.5 mL). Letting the resulting solution stand for 3 h afforded yellow crystals of **8** which could be easily collected by filtration. This procedure afforded **8** in a 81% yield (149 mg). Single crystals of **8** were obtained from CH_2Cl_2 at 0 °C. ^1H NMR (399.51 MHz, $CDCl_3$): δ 7.67 (m, phenylene), 7.39 (broad s). $^{13}C\{^1H\}$ NMR (125.60 MHz, $CDCl_3$): δ 145.88 (Sb*Ph* quaternary), 135.86 (*o*-phenylene), 134.52 (*o*-Sb*Ph*), 131.54 (*o*-phenylene), 130.13 (*p*-Sb*Ph*), 129.29 (*m*-Sb*Ph*); the resonances of the fluorinated carbon atoms were not observed. ^{19}F NMR (375.84 MHz, $CDCl_3$): δ −129.3 (broad d, 4F, $^3J_{F-F}$ = 108.8 Hz), −142.90 (broad s, 2F), −146.41 (broad s, 2F), −156.91 (s, 4F), 160.74 (broad s). Elemental analysis calculated (%) for $C_{58}H_{24}F_{16}O_4Sb_2$: C, 52.29; H, 1.82; found C, 52.59; H, 1.86.

Synthesis of [^{n}Bu$_4$N][8-μ$_2$-F]

A solution of TBAT (40 mg, 0.068 mmol) in CH_2Cl_2 (2 mL) was slowly added to a solution of **8** (90 mg, 0.068 mmol) in CH_2Cl_2 (1 mL). After stirring for 15 min, the resulting solution was brought to dryness under vacuum affording a residue which was washed with Et_2O (2 × 3 mL). This procedure afforded [^{n}Bu$_4$N][**8**-μ$_2$-F] as a yellow solid in a 66% yield (78 mg). Single crystals of [^{n}Bu$_4$N][**8**-μ$_2$-F] were obtained from toluene upon diffusion of pentane. ^1H NMR (399.508 MHz, $CDCl_3$): δ 7.66 (pseudo d, 4H, *m*-Sb*Ph*), 7.52–7.25 (broad m, 20H), 3.05 (m, 8H, TBA–CH_2), 1.58 (broad, 8H, TBA–CH_2), 1.33 (m, 8H, TBA–CH_2), 0.95 (t, 12H, TBA–CH_3, $^3J_{H-H}$ = 7.5 Hz,). $^{13}C\{^1H\}$ NMR (125.60 MHz, CD_3CN): δ 150.16, 150.00, 146.11, 143.31, 143.04, 141.56, 141.37, 135.22 (Sb*Ph* quaternary), 134.57 (*o*-Sb*Ph*), 134.02 (*o*-phenylene), 133.45, 129.99, 129.87 (*p*-Sb*Ph*), 129.59 (*o*-phenylene), 128.75 (*o*-phenylene), 128.34 (*m*-Sb*Ph*), 128.08 (*o*-phenylene), 58.33 (TBA), 23.29 (TBA), 19.24 (TBA), 12.70 (TBA). ^{19}F NMR (375.84 MHz, $CDCl_3$): δ −76.8 (s, 1F, bridging fluoride), −130.5 (pseudo t, 1F, $^3J_{F-F}$ = 15 Hz), −130.9 (pseudo t, 1F, $^3J_{F-F}$ = 15 Hz), −131.8 (pseudo t, 1F, $^3J_{F-F}$ = 15 Hz), −132.3 (pseudo t, 1F, $^3J_{F-F}$ = 15 Hz), −143.7 (pseudo q, 2F, $^3J_{F-F}$ = 23 Hz, $^3J_{F-F}$ = 11 Hz), −147.8 (pseudo q, 2F, $^3J_{F-F}$ = 23 Hz, $^3J_{F-F}$ = 11 Hz), −159.4 (t, 2F, $^3J_{F-F}$ = 23 Hz), −159.7 (t, 2F, $^3J_{F-F}$ = 23 Hz), −164.7 (t, 2F, $^3J_{F-F}$ = 23 Hz), −165.2 (t, 2F, $^3J_{F-F}$ = 23 Hz). Elemental analysis calculated (%) for $C_{74}H_{60}F_{17}NO_4Sb_2$: C, 55.77; H, 3.79; N, 0.88; found C, 56.03; H, 3.84; N, 0.90.

Conflicts of interest

There are no conflicts to declare.

Acknowledgements

Support from the Welch Foundation (Grant A-1423), the National Science Foundation (CHE-1856453), Texas A&M University (Arthur E. Martell Chair of Chemistry), and the Laboratory for Molecular Simulation at Texas A&M University (software and computational resources) is gratefully acknowledged.

References

1 H. Zhao, Y. Kim, G. Park and F. P. Gabbaï, *Tetrahedron*, 2019, **75**, 1123–1129; M. Melaïmi, S. Sole, C.-W. Chiu, H. Wang and F. P. Gabbaï, *Inorg. Chem.*, 2006, **45**, 8136–8143; H. E. Katz, *J. Org. Chem.*, 1985, **50**, 5027–5032.

2 C.-H. Chen and F. P. Gabbaï, *Chem. Sci.*, 2018, **9**, 6210–6218; C.-H. Chen and F. P. Gabbaï, *Angew. Chem., Int. Ed.*, 2018, **57**, 521–525; P. Chen, A. S. Marshall, S.-H. Chi, X. Yin, J. W. Perry and F. Jäkle, *Chem. – Eur. J.*, 2015, **21**, 18237–18247; H. Zhao and F. P. Gabbaï, *Organometallics*, 2012, **31**, 2327–2335; P. Chen and F. Jäkle, *J. Am. Chem. Soc.*, 2011, **133**, 20142–20145; J. K. Day, C. Bresner, N. D. Coombs, I. A. Fallis, L.-L. Ooi and S. Aldridge, *Inorg. Chem.*, 2008, **47**, 793–804; M. H. Lee and F. P. Gabbaï, *Inorg. Chem.*, 2007, **46**, 8132–8138; H. Y. Zhao and F. P. Gabbaï, *Nat. Chem.*, 2010, **2**, 984–990.

3 S. Benz, M. Macchione, Q. Verolet, J. Mareda, N. Sakai and S. Matile, *J. Am. Chem. Soc.*, 2016, **138**, 9093–9096; A. V. Jentzsch, D. Emery, J. Mareda, S. K. Nayak, P. Metrangolo, G. Resnati, N. Sakai and S. Matile, *Nat. Commun.*, 2012, **3**, 905; I. H. A. Badr, M. Diaz, M. F. Hawthorne and L. G. Bachas, *Anal. Chem.*, 1999, **71**, 1371–1377; M. Rothmaier and W. Simon, *Anal. Chim. Acta*, 1993, **271**, 135–141; M. E. Jung and H. Xia, *Tetrahedron Lett.*, 1988, **29**, 297–300; Z. Yan, Z. Zhou, Y. Wu, I. A. Tikhonova and V. B. Shur, *Anal. Lett.*, 2005, **38**, 377–388; N. Chaniotakis, K. Jurkschat, D. Mueller, K. Perdikaki and G. Reeske, *Eur. J. Inorg. Chem.*, 2004, 2283–2288.

4 T. W. Hudnall, C.-W. Chiu and F. P. Gabbaï, *Acc. Chem. Res.*, 2009, **42**, 388–397; E. Galbraith and T. D. James, *Chem. Soc. Rev.*, 2010, **39**, 3831–3842; C. R. Wade, A. E. J. Broomsgrove, S. Aldridge and F. P. Gabbaï, *Chem. Rev.*, 2010, **110**, 3958–3984; *Anion Coordination Chemistry*, ed. K. Bowman-James, A. Bianchi and E. Garcia-Espana, Wiley-VCH Verlag GmbH & Co. KGaA, 2012; H. Zhao, L. A. Leamer and F. P. Gabbaï, *Dalton Trans.*, 2013, **42**, 8164–8178; N. Busschaert, C. Caltagirone, W. Van Rossom and P. A. Gale, *Chem. Rev.*, 2015, **115**, 8038–8155; P. A. Gale, E. N. W. Howe, X. Wu and M. J. Spooner, *Coord. Chem. Rev.*, 2018, **375**, 333–372; L. Schweighauser and H. A. Wegner, *Chem. – Eur. J.*, 2016, **22**, 14094–14103; P. Niermeier, S. Blomeyer, Y. K. J. Bejaoui, J. L. Beckmann, B. Neumann, H.-G. Stammler and N. W. Mitzel, *Angew. Chem., Int. Ed.*, 2019, **58**, 1965–1969.

5 M. Hirai, J. Cho and F. P. Gabbaï, *Chem. – Eur. J.*, 2016, **22**, 6537–6541.

6 M. Hirai and F. P. Gabbaï, *Angew. Chem., Int. Ed.*, 2015, **54**, 1205–1209.

7 C.-H. Chen and F. P. Gabbaï, *Angew. Chem., Int. Ed.*, 2017, **56**, 1799–1804.

8 G. Park and F. P. Gabbaï, *Chem. Sci.*, 2020, **11**, 10107–10112; M. Yang, M. Hirai and F. P. Gabbaï, *Dalton Trans.*, 2019, **48**, 6685–6689; C. R. Wade and F. P. Gabbaï, *Z. Naturforsch., B: J. Chem. Sci.*, 2014, **69**, 1199–1205.

9 C. R. Wade and F. P. Gabbaï, *Organometallics*, 2011, **30**, 4479–4481.

10 M. Baaz, V. Gutmann and O. Kunze, *Monatsh. Chem.*, 1962, **93**, 1142–1161; J. Moc and K. Morokuma, *J. Mol. Struct.*, 1997, **436–437**, 401–418; I. Krossing and I. Raabe, *Chem. – Eur. J.*, 2004, **10**, 5017–5030; A. P. M. Robertson, N. Burford, R. McDonald and M. J. Ferguson, *Angew. Chem., Int. Ed.*, 2014, **53**, 3480–3483; A. P. M. Robertson, S. S. Chitnis, H. A. Jenkins, R. McDonald, M. J. Ferguson and N. Burford, *Chem. – Eur. J.*, 2015, **21**, 7902–7913; S. S. Chitnis, H. A. Sparkes, V. T. Annibale, N. E. Pridmore, A. M. Oliver and I. Manners, *Angew. Chem., Int. Ed.*, 2017, **56**, 9536–9540.

11 G. A. Olah, G. Klopman and R. H. Schlosberg, *J. Am. Chem. Soc.*, 1969, **91**, 3261–3268; G. A. Olah and R. H. Schlosberg, *J. Am. Chem. Soc.*, 1968, **90**, 2726–2727; G. A. Olah, *J. Org. Chem.*, 2005, **70**, 2413–2429.

12 L. A. Körte, J. Schwabedissen, M. Soffner, S. Blomeyer, C. G. Reuter, Y. V. Vishnevskiy, B. Neumann, H.-G. Stammler and N. W. Mitzel, *Angew. Chem., Int. Ed.*, 2017, **56**, 8578–8582; M. Hejda, D. Duvinage, E. Lork, R. Jirásko, A. Lyčka, S. Mebs, L. Dostál and J. Beckmann, *Organometallics*, 2020, **39**, 1202–1212; P. Mehlmann, T. Witteler, L. F. B. Wilm and F. Dielmann, *Nat. Chem.*, 2019, **11**, 1139–1143; J. F. Kögel, D. A. Sorokin, A. Khvorost, M. Scott, K. Harms, D. Himmel, I. Krossing and J. Sundermeyer, *Chem. Sci.*, 2018, **9**, 245–253.

13 L. Greb, *Chem. – Eur. J.*, 2018, **24**, 17881–17896; D. Roth, H. Wadepohl and L. Greb, *Angew. Chem., Int. Ed.*, 2020, **59**, 20930–20934.

14 C. R. Wade, I.-S. Ke and F. P. Gabbaï, *Angew. Chem., Int. Ed.*, 2012, **51**, 478–481; M. Hirai and F. P. Gabbaï, *Chem. Sci.*, 2014, **5**, 1886–1893; M. Hirai, M. Myahkostupov, F. N. Castellano and F. P. Gabbaï, *Organometallics*, 2016, **35**, 1854–1860.

15 G. Park, D. J. Brock, J.-P. Pellois and F. P. Gabbaï, *Chem*, 2019, **5**, 2215–2227; G. Park and F. P. Gabbaï, *Angew. Chem., Int. Ed.*, 2020, **59**, 5298–5302.

16 T. J. Taylor, C. N. Burress and F. P. Gabbaï, *Organometallics*, 2007, **26**, 5252–5263.

17 V. C. Williams, W. E. Piers, W. Clegg, M. R. J. Elsegood, S. Collins and T. B. Marder, *J. Am. Chem. Soc.*, 1999, **121**, 3244–3245.

18 S. P. Lewis, J. Chai, S. Collins, T. J. J. Sciarone, L. D. Henderson, C. Fan, M. Parvez and W. E. Piers, *Organometallics*, 2009, **28**, 249–263.

19 J. L. Kiplinger and T. G. Richmond, *J. Am. Chem. Soc.*, 1996, **118**, 1805–1806.

20 A. W. Addison, T. N. Rao, J. Reedijk, J. van Rijn and G. C. Verschoor, *J. Chem. Soc., Dalton Trans.*, 1984, 1349–1356.

21 D. Tofan and F. P. Gabbaï, *Chem. Sci.*, 2016, **7**, 6768–6778; M. Yang, D. Tofan, C.-H. Chen, K. M. Jack and F. P. Gabbaï, *Angew. Chem., Int. Ed.*, 2018, **57**, 13868–13872.

22 R. R. Holmes, R. O. Day, V. Chandrasekhar and J. M. Holmes, *Inorg. Chem.*, 1987, **26**, 157–163.

23 I.-S. Ke, M. Myahkostupov, F. N. Castellano and F. P. Gabbaï, *J. Am. Chem. Soc.*, 2012, **134**, 15309–15311.
24 S. Solé and F. P. Gabbaï, *Chem. Commun.*, 2004, 1284–1285.
25 D. Zhang, S. J. Rettig, J. Trotter and F. Aubke, *Inorg. Chem.*, 1996, **35**, 6113–6130.
26 W. Levason, C. A. McAuliffe and S. G. Murray, *J. Organomet. Chem.*, 1975, **88**, 171–174.
27 A. L. Liberman-Martin, R. G. Bergman and T. D. Tilley, *J. Am. Chem. Soc.*, 2015, **137**, 5328–5331.
28 M. Nunn, D. B. Sowerby and D. M. Wesolek, *J. Organomet. Chem.*, 1983, **251**, C45–C46.
29 M. J. Frisch, G. W. Trucks, H. B. Schlegel, G. E. Scuseria, M. A. Robb, J. R. Cheeseman, G. Scalmani, V. Barone, B. Mennucci, G. A. Petersson, H. Nakatsuji, M. Caricato, X. Li, H. P. Hratchian, A. F. Izmaylov, J. Bloino, G. Zheng, J. L. Sonnenberg, M. Hada, M. Ehara, K. Toyota, R. Fukuda, J. Hasegawa, M. Ishida, T. Nakajima, Y. Honda, O. Kitao, H. Nakai, T. Vreven, J. A. Montgomery, Jr., J. E. Peralta, F. Ogliaro, M. Bearpark, J. J. Heyd, E. Brothers, K. N. Kudin, V. N. Staroverov, R. Kobayashi, J. Normand, K. Raghavachari, A. Rendell, J. C. Burant, S. S. Iyengar, J. Tomasi, M. Cossi, N. Rega, J. M. Millam, M. Klene, J. E. Knox, J. B. Cross, V. Bakken, C. Adamo, J. Jaramillo, R. Gomperts, R. E. Stratmann, O. Yazyev, A. J. Austin, R. Cammi, C. Pomelli, J. W. Ochterski, R. L. Martin, K. Morokuma, V. G. Zakrzewski, G. A. Voth, P. Salvador, J. J. Dannenberg, S. Dapprich, A. D. Daniels, Ö. Farkas, J. B. Foresman, J. V. Ortiz, J. Cioslowski and D. J. Fox, *Gaussian 09, Revision B.01*, Gaussian, Inc., Wallingford, CT, 2009.
30 A. D. Becke, *J. Chem. Phys.*, 1993, **98**, 5648–5652; C. T. Lee, W. T. Yang and R. G. Parr, *Phys. Rev. B: Condens. Matter Mater. Phys.*, 1988, **37**, 785–789; S. H. Vosko, L. Wilk and M. Nusair, *Can. J. Phys.*, 1980, **58**, 1200–1211; P. J. Stephens, F. J. Devlin, C. F. Chabalowski and M. J. Frisch, *J. Phys. Chem.*, 1994, **98**, 11623–11627.
31 K. A. Peterson, D. Figgen, E. Goll, H. Stoll and M. Dolg, *J. Chem. Phys.*, 2003, **119**, 11113–11123; K. A. Peterson, *J. Chem. Phys.*, 2003, **119**, 11099–11112; K. A. Peterson, B. C. Shepler, D. Figgen and H. Stoll, *J. Phys. Chem. A*, 2006, **110**, 13877–13883.
32 M. M. Francl, W. J. Pietro, W. J. Hehre, J. S. Binkley, M. S. Gordon, D. J. DeFrees and J. A. Pople, *J. Chem. Phys.*, 1982, **77**, 3654–3665; A. D. McLean and G. S. Chandler, *J. Chem. Phys.*, 1980, **72**, 5639–5648.
33 G. A. Petersson, A. Bennett, T. G. Tensfeldt, M. A. Al-Laham, W. A. Shirley and J. Mantzaris, *J. Chem. Phys.*, 1988, **89**, 2193–2218; G. A. Petersson and M. A. Al-Laham, *J. Chem. Phys.*, 1991, **94**, 6081–6090.
34 R. Ditchfield, W. J. Hehre and J. A. Pople, *J. Chem. Phys.*, 1971, **54**, 724–728; W. J. Hehre, R. Ditchfield and J. A. Pople, *J. Chem. Phys.*, 1972, **56**, 2257–2261.
35 D. Harrison, M. Stacey, R. Stephens and J. C. Tatlow, *Tetrahedron*, 1963, **19**, 1893–1901.